Angiotensin AT_{1A} receptors on leptin receptor–expressing cells control resting metabolism

Kristin E. Claflin,[1] Jeremy A. Sandgren,[1] Allyn M. Lambertz,[2] Benjamin J. Weidemann,[1] Nicole K. Littlejohn,[1] Colin M.L. Burnett,[1] Nicole A. Pearson,[1] Donald A. Morgan,[1] Katherine N. Gibson-Corley,[2,3] Kamal Rahmouni,[1,3,4,5,6] and Justin L. Grobe[1,3,4,5,6]

[1]Department of Pharmacology, [2]Department of Pathology, [3]University of Iowa Health Care (UIHC) Center for Hypertension Research, [4]Obesity Research and Education Initiative, [5]François M. Abboud Cardiovascular Research Center, and [6]Fraternal Order of Eagles Diabetes Research Center, University of Iowa, Iowa City, Iowa, USA.

Leptin contributes to the control of resting metabolic rate (RMR) and blood pressure (BP) through its actions in the arcuate nucleus (ARC). The renin-angiotensin system (RAS) and angiotensin AT_1 receptors within the brain are also involved in the control of RMR and BP, but whether this regulation overlaps with leptin's actions is unclear. Here, we have demonstrated the selective requirement of the AT_{1A} receptor in leptin-mediated control of RMR. We observed that AT_{1A} receptors colocalized with leptin receptors (LEPRs) in the ARC. Cellular coexpression of AT_{1A} and LEPR was almost exclusive to the ARC and occurred primarily within neurons expressing agouti-related peptide (AgRP). Mice lacking the AT_{1A} receptor specifically in LEPR-expressing cells failed to show an increase in RMR in response to a high-fat diet and deoxycorticosterone acetate–salt (DOCA-salt) treatments, but BP control remained intact. Accordingly, loss of RMR control was recapitulated in mice lacking AT_{1A} in AgRP-expressing cells. We conclude that angiotensin activates divergent mechanisms to control BP and RMR and that the brain RAS functions as a major integrator for RMR control through its actions at leptin-sensitive AgRP cells of the ARC.

Introduction

The renin-angiotensin system (RAS) contributes to blood pressure (BP) and fluid balance control. Selected tissues contain an autocrine/paracrine RAS, in which local synthesis of angiotensin II (ANG II) and its receptors regulate regional function (1). All components of the RAS have been documented in specific brain nuclei, and the brain RAS has been implicated in BP control. Both ANG type 1 (AT_1) and type 2 (AT_2) receptors are expressed in the brain, and it is believed that the majority of the central effects of ANG II on cardiovascular function are mediated through the AT_1 receptor in humans and its AT_{1A} homolog in rodents (2, 3). Interestingly, the AT_1 receptor is robustly expressed in the arcuate nucleus (ARC) (4–6), a site implicated in metabolic control but less appreciated in cardiovascular control. Although microinjection of exogenous ANG II into the ARC increases mean arterial pressure (7), it is not known whether ANG II signaling in the ARC is necessary for BP regulation. The role of ANG II in the ARC therefore remains unclear.

In contrast, there is a well-defined role for leptin in the ARC in the control of both BP and energy balance. Leptin action at proopiomelanocortin (POMC) neurons of the ARC is critical for BP regulation (8), and both POMC and agouti-related peptide (AgRP) neurons mediate the metabolic effects of leptin in the ARC. While the brain RAS has been implicated in the control of selected aspects of energy balance including food intake and energy expenditure, the specific brain regions involved and the neurocircuitry that mediates these effects are unknown (9, 10).

Here, we examined the concept that AT_{1A} receptors in the ARC are involved in energy homeostasis. Specifically, we document a critical role for AT_{1A} expressed in cells that also express the leptin receptor (LEPR) in resting metabolic rate (RMR) control. In addition, we document a specific directionality of the leptin-AT_{1A} interaction and establish a primary role for AT_{1A} within the subset of LEPR-expressing cells that also express AgRP. These findings document a local autocrine/paracrine leptin-RAS interaction within the ARC, clarify the divergent control of BP versus RMR by the ARC, and highlight a major integrative role for the ARC RAS in RMR control.

Results

Brain ANG II stimulates RMR via AT_1 receptors. To establish a primary role for AT_1 receptors in the RMR-stimulating effects of central ANG II, RMR was determined by respirometry in animals after i.c.v. infusion of either artificial cerebral spinal fluid (aCSF) or ANG II. Mice receiving i.c.v. ANG II exhibited a significant increase in RMR compared with aCSF-treated animals after 10 days of treatment (Figure 1, A and B), with no significant alterations in the respiratory exchange ratio (RER) (Figure 1C). Mice were also subsequently treated with losartan in their drinking water for 7 days (0.8 mg/ml). While mice that received i.c.v. aCSF did not show any change in RMR with losartan, mice treated with i.c.v. ANG II showed a significant reduction in RMR (Figure 1D). Taken together, these data support the idea that central ANG II signaling stimulates RMR via the ANG II AT_1 receptor; however, it remains unclear which AT_1 receptors in the brain are important for this control.

LEPR and AT_{1A} colocalize within the ARC. We examined expression patterns of both LEPR and AT_{1A} by using the NZ44-transgenic mouse, which expresses GFP inserted into the *AT1a* locus in a recombineered BAC transgene (11), and mice that conditionally

Conflict of interest: The authors have declared that no conflict of interest exists.
Submitted: May 18, 2016; **Accepted:** January 12, 2017.
Reference information: *J Clin Invest*. 2017;127(4):1414–1424.
https://doi.org/10.1172/JCI88641.

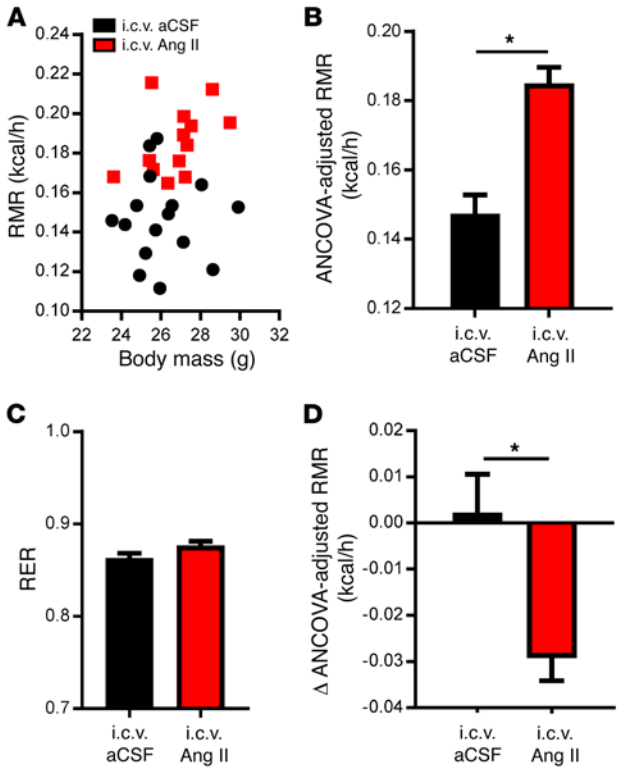

Figure 1. Intracerebroventricular ANG II stimulates the RMR via AT_{1A} receptors. (**A**–**C**) RMR versus body mass (**A**), ANCOVA-adjusted RMR (**B**), and RER (**C**) of C57BL/6J mice after 10 days of i.c.v. aCSF or ANG II treatment (n = 16 aCSF-treated mice; n = 13 ANG II–treated mice). (**D**) Change in ANCOVA-adjusted RMR in mice given i.c.v. aCSF or ANG II after 7 days of losartan treatment (n = 6 aCSF-treated mice; n =11 ANG II–treated mice). Data represent the mean ± SEM. *P < 0.05, by Student's t test.

express a red fluorescent reporter after Cre-mediated recombination in LEPR-expressing cells (*Lepr-Cre ROSA-stop^{flox}-tdTomato*) (12–14). We identified LEPR- and AT_{1A}-coexpressing cells by the colocalization of red and green fluorescence in the brain. Cells expressing both receptors were abundant in the ARC of the hypothalamus, with minimal colocalization in the lateral hypothalamus, dorsomedial hypothalamus, and nucleus tractus solitarii (Figure 2A). Cells expressing either, but not both, receptors were detected in other regions. These findings support the notion of a primary colocalization of LEPR and AT_{1A} within the ARC.

AT_{1A} in leptin-sensitive cells is necessary for energy homeostasis. To determine whether ANG II signaling specifically in leptin-sensitive cells is involved in the control of energy balance, we created a transgenic mouse model that lacks the AT_{1A} receptor in any cell expressing the long (b) signaling form of LEPR (*AT1a$^{fl/fl}$ Lepr-Cre* mice, referred to hereafter as $AT_{1A}^{LepR\text{-}KO}$ mice). Cre-recombinase activity was confirmed by PCR amplification of the *AT1a* gene using primers that generate different-sized products, depending on Cre-mediated recombination. Cre-recombinase–mediated recombination of the *AT1a* gene was detected in the supraoptic nucleus (SON) and the ARC, but not in the subfornical organ (SFO), paraventricular nucleus (PVN), or cortex, probably because of the low abundance of *Lepr-Cre*–expressing cells in these regions (Figure 2B). Critically, with the exception of lung tissue in which *AT1a* expression was already very low at baseline, we observed no changes in *AT1a* mRNA expression in peripheral tissues (Figure 2C). Thus, the physiological phenotypes observed in $AT_{1A}^{LepR\text{-}KO}$ mice were likely due to the loss of ANG II receptor signaling on LEPR-containing cells within the ventromedial ARC. Importantly, the loss of AT_{1A} receptors on LEPR-containing cells does not block leptin signaling, as phosphorylation of STAT3 (p-STAT3) was preserved in the ARC of $AT_{1A}^{LepR\text{-}KO}$ mice in response to leptin (Figure 2D).

Next, we assessed whether $AT_{1A}^{LepR\text{-}KO}$ mice have altered energy homeostasis. Under ad libitum chow-fed conditions (Teklad Diet 7013; 18% kcal from fat), $AT_{1A}^{LepR\text{-}KO}$ mice exhibited normal body mass and fat mass (Figure 3, A and B). When maintained on a chow diet, these mice had normal food intake, digestive efficiency, physical activity, RMR, and brown adipose tissue (BAT) uncoupling protein 1 (*Ucp1*) mRNA levels (Figure 3, C–G). While both control and $AT_{1A}^{LepR\text{-}KO}$ mice responded to 5 weeks of 45% high-fat diet (HFD) (OpenSource D12451) treatment, with elevations in body weight and fat mass, $AT_{1A}^{LepR\text{-}KO}$ mice gained significantly more weight and fat mass than did their control littermates (Figure 3, A and B). There were no significant differences in food intake (Figure 3C) or digestive efficiency (Figure 3D) between $AT_{1A}^{LepR\text{-}KO}$ and littermate control mice during HFD treatment, indicating a normal total daily energy input. Whereas control littermates responded to HFD treatment with a significant increase in RMR after just 2 weeks of treatment (Figure 3F), $AT_{1A}^{LepR\text{-}KO}$ mice failed to show RMR stimulation, and the induction of BAT *Ucp1* expression was severely compromised (Figure 3G). Of critical importance, the lack of RMR stimulation in response to an HFD occurred prior to significant alterations in body weight and composition, consistent with the concept that the reduced increase in RMR is causal for the increased body adiposity observed in $AT_{1A}^{LepR\text{-}KO}$ mice.

Sympathetic nerve activity (SNA) responses to leptin are attenuated in mice with global AT_{1A} disruption and in rats administered i.c.v. losartan (15), suggesting that central ANG II signaling through AT_{1A} receptors is required for leptin action. Consistent with this hypothesis, the BAT SNA response to leptin was significantly attenuated in $AT_{1A}^{LepR\text{-}KO}$ mice (Figure 3H). The reduction in leptin-stimulated BAT SNA in $AT_{1A}^{LepR\text{-}KO}$ mice probably explains the loss of RMR and UCP1 responses to HFD in these animals and the subsequent elevation in fat mass, as it has been previously shown that enhanced SNA is necessary to counteract weight gain following high caloric intake (13). Thus, we conclude that AT_{1A} receptors expressed in leptin-sensitive cells are required to mediate the RMR response to HFD and leptin via activation of thermogenic SNA.

AT_{1A} receptors in LEPR-expressing cells selectively mediate RMR but not BP. The DOCA-salt model (deoxycorticosterone acetate plus a high dietary sodium load) of hypertension is a well-established model of low-renin hypertension mechanistically involving brain ANG II and AT_{1A} receptors (16–18). It is notable that DOCA-salt also robustly stimulates RMR, an effect that also requires brain AT_{1A} receptors (19). However, it is not known whether RMR and BP responses are mediated by AT_{1A} receptors on the same population of cells in the brain. Given the HFD results obtained above, we asked whether the RMR responses to DOCA-salt required AT_{1A} receptors expressed in LEPR-expressing cells and whether these cells also mediate the BP response. Control litter-

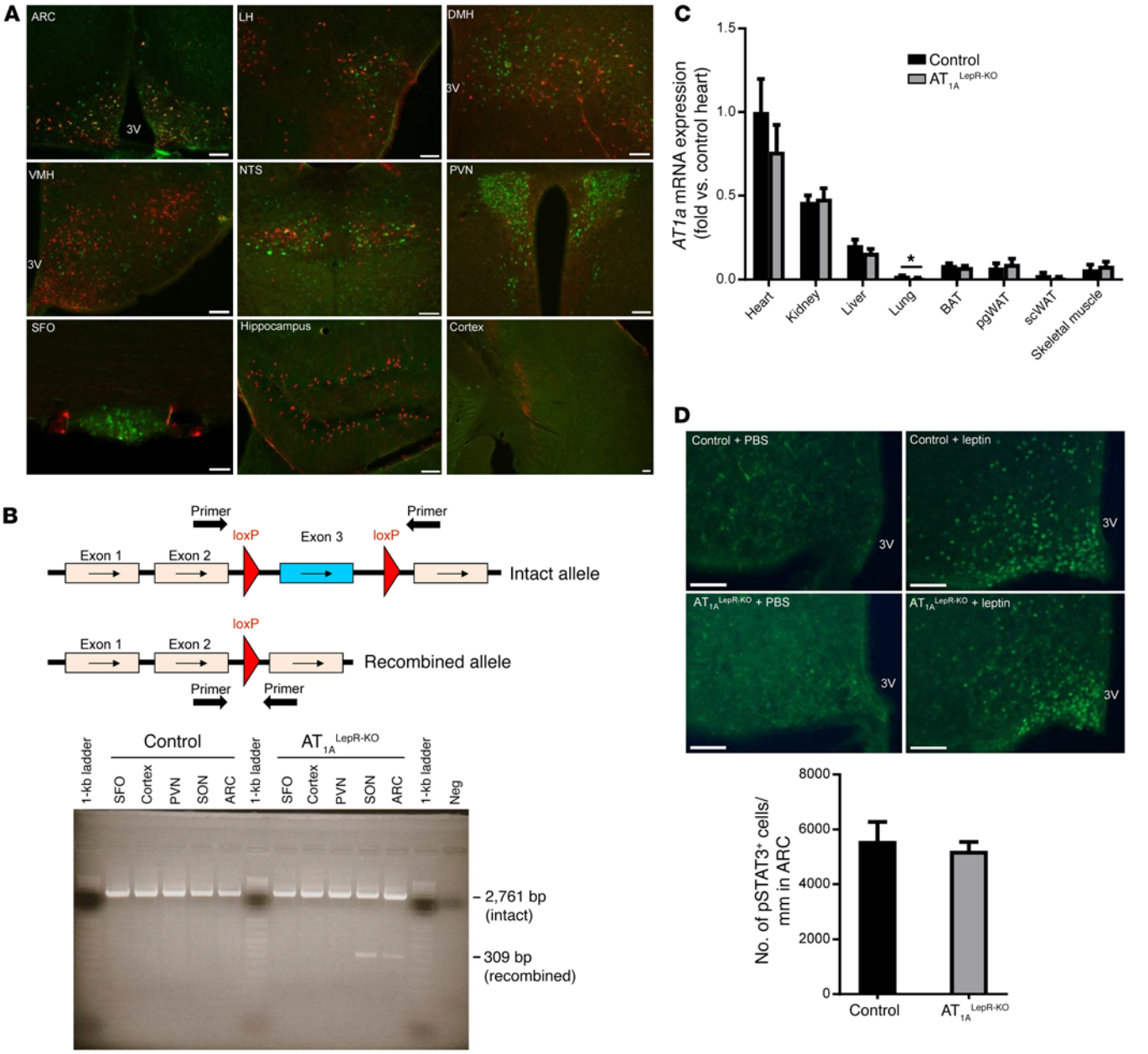

Figure 2. AT_{1A} and LEPR colocalize within cells in the ARC. (**A**) Representative photomicrographs of AT_{1A} and LEPR expression in various brain regions including the ARC, lateral hypothalamus (LH), dorsomedial hypothalamus (DMH), ventromedial hypothalamus (VMH), nucleus tractus solitarii (NTS), PVN, SFO, hippocampus, and cortex. Scale bars: 100 μm. (**B**) Primers for the detection of genetic recombination of the *AT1a* gene span the floxed region. Intact and recombined *AT1a*$^{fl/fl}$ gene expression in the SFO, cortex, PVN, SON, and ARC of control and $AT_{1A}^{LepR\text{-}KO}$ animals. (**C**) AT_{1A} expression in peripheral tissues, including heart, kidney, liver, lung, BAT, perigonadal white adipose tissue (pgWAT), s.c. WAT (scWAT) and skeletal muscle of control and $AT_{1A}^{LepR\text{-}KO}$ mice (n = 6/group). Data represent the mean ± SEM. *$P < 0.05$, by Tukey's multiple comparisons procedure. (**D**) ARC p-STAT3 expression following i.p. PBS or leptin (1 μg/g) in control and $AT_{1A}^{LepR\text{-}KO}$ mice after 2 weeks of HFD treatment (PBS-treated control mice; n = 3 leptin-treated control mice; PBS-treated $AT_{1A}^{LepR\text{-}KO}$ mouse; n = 6 leptin-treated $AT_{1A}^{LepR\text{-}KO}$ mice). Scale bars: 75 μm. Data represent the mean ± SEM. 3V, third ventricle.

mates responded to DOCA-salt treatment with a significant elevation in RMR, but this increase was markedly blunted in $AT_{1A}^{LepR\text{-}KO}$ mice (Figure 4A; genotype-DOCA interaction $P = 0.02$). This suggests that the RMR response to both leptin (HFD) and ANG II (DOCA-salt) is impaired in $AT_{1A}^{LepR\text{-}KO}$ mice. In contrast, there was a normal increase in BP (Figure 4B) and reduction in heart rate (Figure 4C) in $AT_{1A}^{LepR\text{-}KO}$ mice in response to DOCA-salt. Taken together, these results are consistent with a selective role for AT_{1A} receptors in leptin-sensitive cells for metabolic, but not cardiovascular, control physiology.

A unidirectional interaction between AT_{1A} and LEPR in RMR control. To elucidate the directionality of the central interaction between leptin and ANG II in RMR control, we next examined the effects of stimulating the brain RAS in LEPR-deficient animals (*db/db* mice). At baseline, *db/db* mice had significant elevations in body and fat mass as previously reported (Figure 4, D and E). Fol-

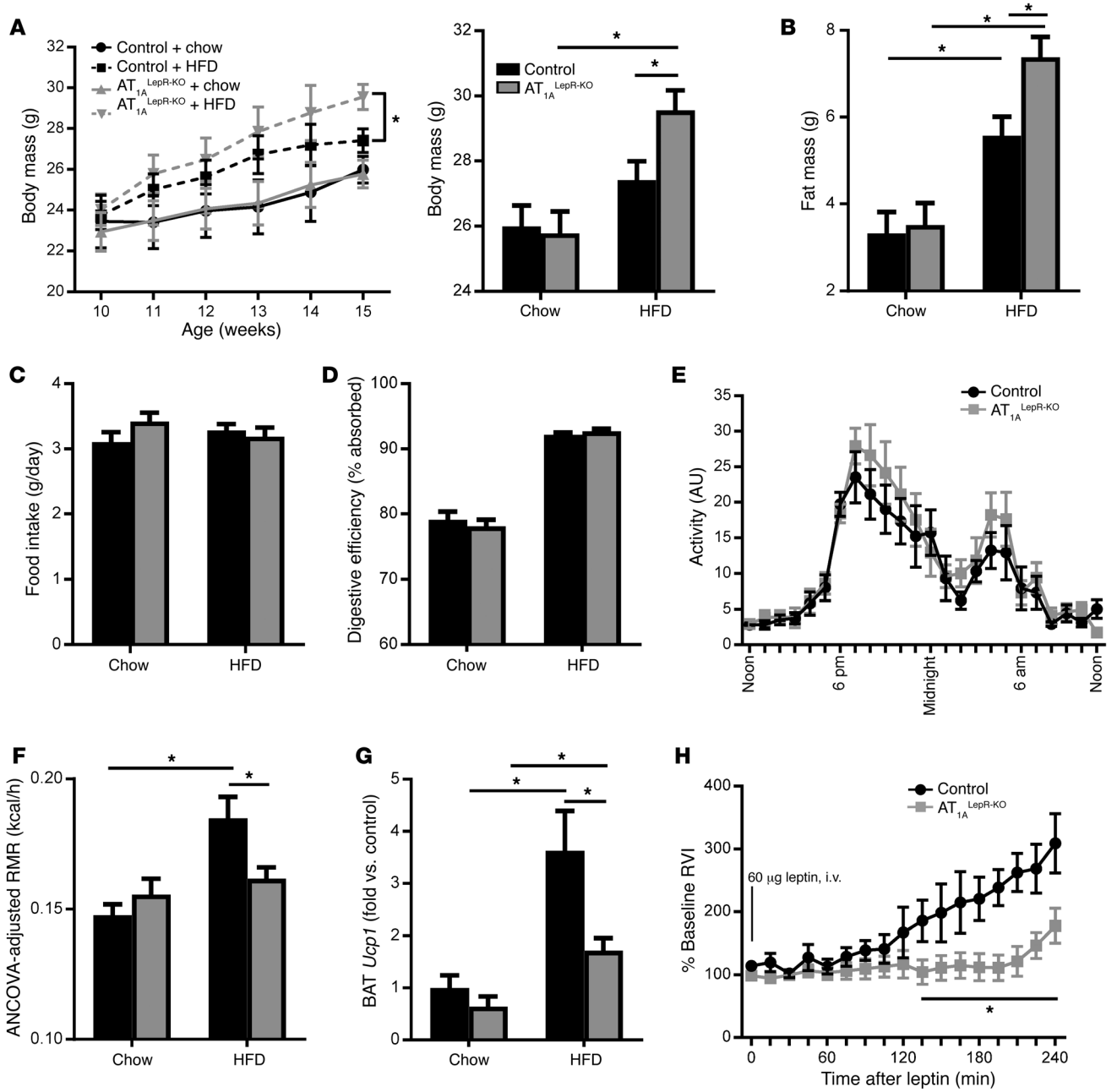

Figure 3. $AT_{1A}^{LepR\text{-}KO}$ mice exhibit impaired responses to an HFD and leptin. (**A**–**D**) Body mass (**A**) (n = 28 chow-fed control mice; n = 35 HFD-fed control mice; n = 26 chow-fed $AT_{1A}^{LepR\text{-}KO}$ mice; n = 31 HFD-fed $AT_{1A}^{LepR\text{-}KO}$ mice); fat mass (**B**) (n = 28 chow-fed control mice; n = 35 HFD-fed control mice; n = 26 chow-fed $AT_{1A}^{LepR\text{-}KO}$ mice; n = 31 HFD-fed $AT_{1A}^{LepR\text{-}KO}$ mice); home cage food intake (**C**) (n = 12 chow-fed control mice; n = 29 HFD-fed control mice; n = 15 chow-fed $AT_{1A}^{LepR\text{-}KO}$ mice; n = 14 HFD-fed $AT_{1A}^{LepR\text{-}KO}$ mice); and digestive efficiency (**D**) (n = 5/group) of control and $AT_{1A}^{LepR\text{-}KO}$ mice on a chow diet or after 5 weeks of 45% HFD treatment. (**E**) Physical activity of control and $AT_{1A}^{LepR\text{-}KO}$ mice on a chow diet (n = 10 control mice; n = 9 $AT_{1A}^{LepR\text{-}KO}$ mice). (**F** and **G**) ANCOVA-adjusted RMR (**F**) (n = 13 chow-fed control mice; n = 22 HFD-fed control mice; n = 15 chow-fed $AT_{1A}^{LepR\text{-}KO}$ mice; n = 12 HFD-fed $AT_{1A}^{LepR\text{-}KO}$ mice) and BAT *Ucp1* expression (**G**) (n = 4 chow-fed control mice; n = 4 HFD-fed control mice; n = 5 chow-fed $AT_{1A}^{LepR\text{-}KO}$ mice; n = 8 HFD-fed $AT_{1A}^{LepR\text{-}KO}$ mice) in control and $AT_{1A}^{LepR\text{-}KO}$ mice on a chow diet or after 2 weeks of HFD treatment. (**H**) Changes in BAT SNA following i.v. administration of leptin (60 μg) in control and $AT_{1A}^{LepR\text{-}KO}$ mice (n = 6 control mice; n = 5 $AT_{1A}^{LepR\text{-}KO}$ mice). RVI, rectified/integrated voltage. Data represent the mean ± SEM. *$P < 0.05$, by Tukey's multiple comparisons procedure.

lowing DOCA-salt RMR stimulation, both control and *db/db* mice responded with significant elevations in RMR (Figure 4F). Consistent with an increase in RMR, DOCA-salt–treated *db/db* mice exhibited a significant reduction in fat mass (Figure 4E). This, in combination with the findings above, leads to the conclusion that the metabolic effects of leptin require functional AT_{1A} receptors on LEPR-containing cells, while the RMR effects of brain ANG II do not require functional leptin signaling. We conclude that there is a specific directionality to the central interaction between leptin and ANG II in RMR control. Moreover, BP responses to DOCA-

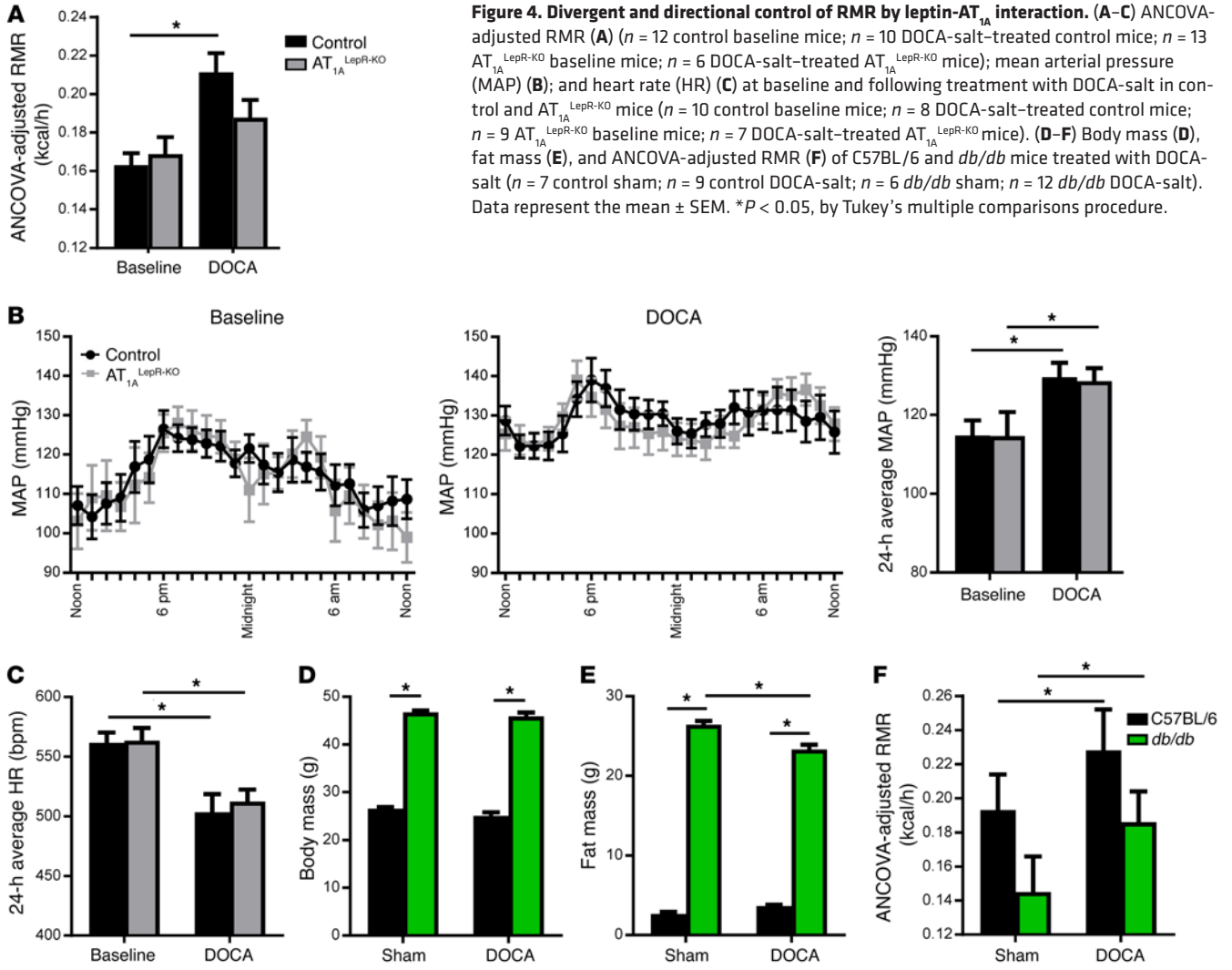

Figure 4. Divergent and directional control of RMR by leptin-AT_{1A} interaction. (**A**–**C**) ANCOVA-adjusted RMR (**A**) (n = 12 control baseline mice; n = 10 DOCA-salt–treated control mice; n = 13 $AT_{1A}^{LepR\text{-}KO}$ baseline mice; n = 6 DOCA-salt–treated $AT_{1A}^{LepR\text{-}KO}$ mice); mean arterial pressure (MAP) (**B**); and heart rate (HR) (**C**) at baseline and following treatment with DOCA-salt in control and $AT_{1A}^{LepR\text{-}KO}$ mice (n = 10 control baseline mice; n = 8 DOCA-salt–treated control mice; n = 9 $AT_{1A}^{LepR\text{-}KO}$ baseline mice; n = 7 DOCA-salt–treated $AT_{1A}^{LepR\text{-}KO}$ mice). (**D**–**F**) Body mass (**D**), fat mass (**E**), and ANCOVA-adjusted RMR (**F**) of C57BL/6 and *db/db* mice treated with DOCA-salt (n = 7 control sham; n = 9 control DOCA-salt; n = 6 *db/db* sham; n = 12 *db/db* DOCA-salt). Data represent the mean ± SEM. *$P < 0.05$, by Tukey's multiple comparisons procedure.

salt are preserved in *db/db* mice (20), further supporting a model of divergent BP and RMR control by the brain RAS, involving AT_{1A} receptors in distinct neural pathways.

Reduced AgRP and normal POMC responses to HFD in the ARC in $AT_{1A}^{LepR\text{-}KO}$ mice. To determine whether AT_{1A} is localized to a specific subset of LEPR-expressing cells of the ARC, we first examined the expression of *Pomc* and *Agrp* genes within this brain region in $AT_{1A}^{LepR\text{-}KO}$ and littermate control mice under chow- and HFD-fed conditions. Five weeks of HFD feeding caused a significant increase in POMC expression in the hypothalamus of both $AT_{1A}^{LepR\text{-}KO}$ and control littermate mice (Figure 5A). In contrast, HFD feeding caused a significant suppression of hypothalamic *Agrp* mRNA expression in control mice, but no significant suppression was observed in $AT_{1A}^{LepR\text{-}KO}$ mice (Figure 5B). These data support the concept that loss of AT_{1A} in LEPR-expressing cells has the specific effect of modulating the function of AgRP, but possibly not POMC, neurons of the hypothalamus.

AT_{1A} disruption in AgRP-expressing cells specifically interrupts RMR control. We next investigated the colocalization of AT_{1A} receptors with POMC and AgRP neurons. To determine whether POMC neurons express the AT_{1A} receptor, we immunostained brain tissue from NZ44 mice for adrenocorticotropin (ACTH), a cleavage product of the *Pomc* gene and a marker for POMC neurons. To determine whether AgRP neurons express the AT_{1A} receptor, mice expressing tdTomato under control of the *Agrp* promoter (*Agrp-Cre ROSA-stop^{flox}-tdTomato* mice) were bred with NZ44 mice. While POMC neurons do not appear to express the AT_{1A} receptor, we observed a significant localization of the AT_{1A} receptor on AgRP neurons (Figure 5C). These data are consistent with RNA-sequencing data demonstrating expression of AT_{1A} receptors on AgRP, but not POMC, neurons isolated by laser-capture microdissection (21). To complement this reporter-based method, we also used FISH (RNAscope) to examine the colocalization of endogenous *AT1a*, *Pomc*, and *Agrp* mRNA transcripts in the ARC of WT C57BL/6J mice. As expected, we detected *AT1a* transcripts in cells also expressing AgRP, but not in cells expressing POMC (Figure 5D and Supplemental Data; supplemental material available online with this article; https://doi.org/10.1172/JCI88641DS1).

α-Melanocyte–stimulating hormone action on second-order neurons is suppressed in $AT_{1A}^{LepR\text{-}KO}$ mice. We next hypothesized that the loss of AT_{1A} in AgRP neurons of $AT_{1A}^{LepR\text{-}KO}$ mice would result in disinhibited inhibitory tone to second-order neurons and thereby attenuated RMR responses to exogenous α-melanocyte–stimulating hormone (αMSH). To test this concept, we administered

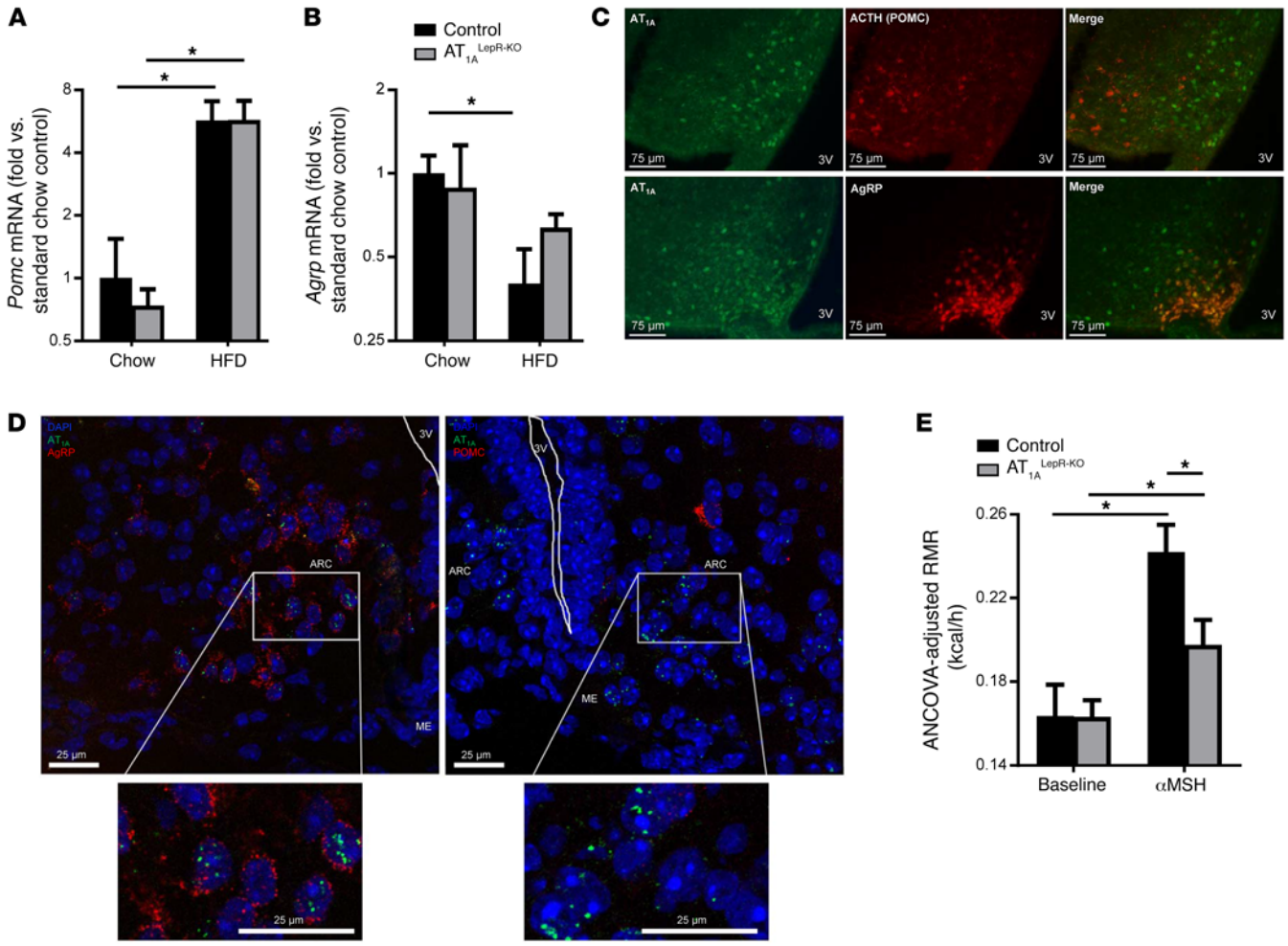

Figure 5. AT_{1A} in AgRP neurons. (**A** and **B**) Hypothalamic *Pomc* (**A**) and *Agrp* (**B**) mRNA expression in control and $AT_{1A}^{LepR\text{-}KO}$ mice on a chow diet or after 5 weeks of a 45% HFD (n = 12 chow-fed control mice; n = 4 HFD-fed control mice; n = 4 chow-fed $AT_{1A}^{LepR\text{-}KO}$ mice; n = 6 HFD-fed $AT_{1A}^{LepR\text{-}KO}$ mice). (**C**) Representative photomicrographs of AT_{1A} receptor and ACTH (POMC) or AgRP in the ARC of chow-fed *Lepr-Cre ROSA-stop^{flox}-tdTomato* NZ44 animals (scale bars: 75 μm). (**D**) FISH for *AT1a*, *Pomc*, and *Agrp* mRNA transcripts in the ARC of WT C57BL/6J mice (scale bars: 25 μm). (**E**) ANCOVA-adjusted RMR at baseline and in response to i.p. administration of [Nle^4_D-Phe^7]-αMSH (4.5 μg/g) in control and $AT_{1A}^{LepR\text{-}KO}$ mice (n = 3 control baseline; n = 3 control αMSH-treated mice; n = 7 chow-fed $AT_{1A}^{LepR\text{-}KO}$ mice; n = 7 αMSH-treated $AT_{1A}^{LepR\text{-}KO}$ mice). *$P < 0.05$, by Tukey's multiple comparisons procedure.

[Nle^4_D-Phe^7]-αMSH, an analog of αMSH that has been demonstrated to stimulate RMR after peripheral administration (22), to both control and $AT_{1A}^{LepR\text{-}KO}$ mice and examined acute RMR responses. As expected, while both control littermates and $AT_{1A}^{LepR\text{-}KO}$ mice responded to acute αMSH treatment with significant elevations in RMR, this response was blunted in $AT_{1A}^{LepR\text{-}KO}$ mice as compared with that in control animals (Figure 5E). Importantly, a volume-matched injection of 0.9% saline had no effect on RMR (data not shown). These results indicate that loss of AT_{1A} receptors in leptin-sensitive cells interferes with the action of αMSH on second-order neurons and thereby leptin-mediated control of SNA and RMR. We speculate that AT_{1A} in LEPR-expressing cells is required to disinhibit SNA and RMR activation by αMSH signaling.

Specific disruption of AT_{1A} in AgRP neurons of $AT_{1A}^{AgRP\text{-}KO}$ mice. Given the colocalization of AT_{1A} and AgRP within the ARC, we explored the functional role of AT_{1A} within AgRP neurons in RMR control in mice lacking AT_{1A} receptors specifically in AgRP-expressing cells ($AT_{1A}^{AgRP\text{-}KO}$ mice). Mice expressing Cre-recombinase via the *Agrp* promoter (*Agrp-Cre*) (23) were bred with mice harboring the conditional *AT1a* allele. Like $AT_{1A}^{LepR\text{-}KO}$ mice, $AT_{1A}^{AgRP\text{-}KO}$ mice exhibited a normal RMR when maintained on a standard chow diet (Figure 6A) but had suppressed BAT SNA in response to i.c.v. injection of leptin (Figure 6B) and suppressed RMR responses to acute αMSH injection (Figure 6C). Notably, these effects were similar to those observed in $AT_{1A}^{LepR\text{-}KO}$ mice. Together, we conclude that AT_{1A} receptors, localized to the subset of AgRP- and LEPR-expressing cells within the ARC, are critically and specifically involved in the control of RMR.

Disinhibition of GABA in $AT_{1A}^{AgRP\text{-}KO}$ mice. Finally, we investigated possible mediators of AT_{1A} signaling, focusing on mechanisms that have been documented in AgRP neurons such as GABA signaling. Previously, it was established that disruption of the LEPR in vesicular GABA transporter–expressing (VGAT-expressing) cells induces obesity (24), similar to that seen in $AT_{1A}^{LepR\text{-}KO}$ mice. Moreover, genetic disruption of *VGAT* within AgRP neurons elicited phenotypes opposite those of $AT_{1A}^{LepR\text{-}KO}$

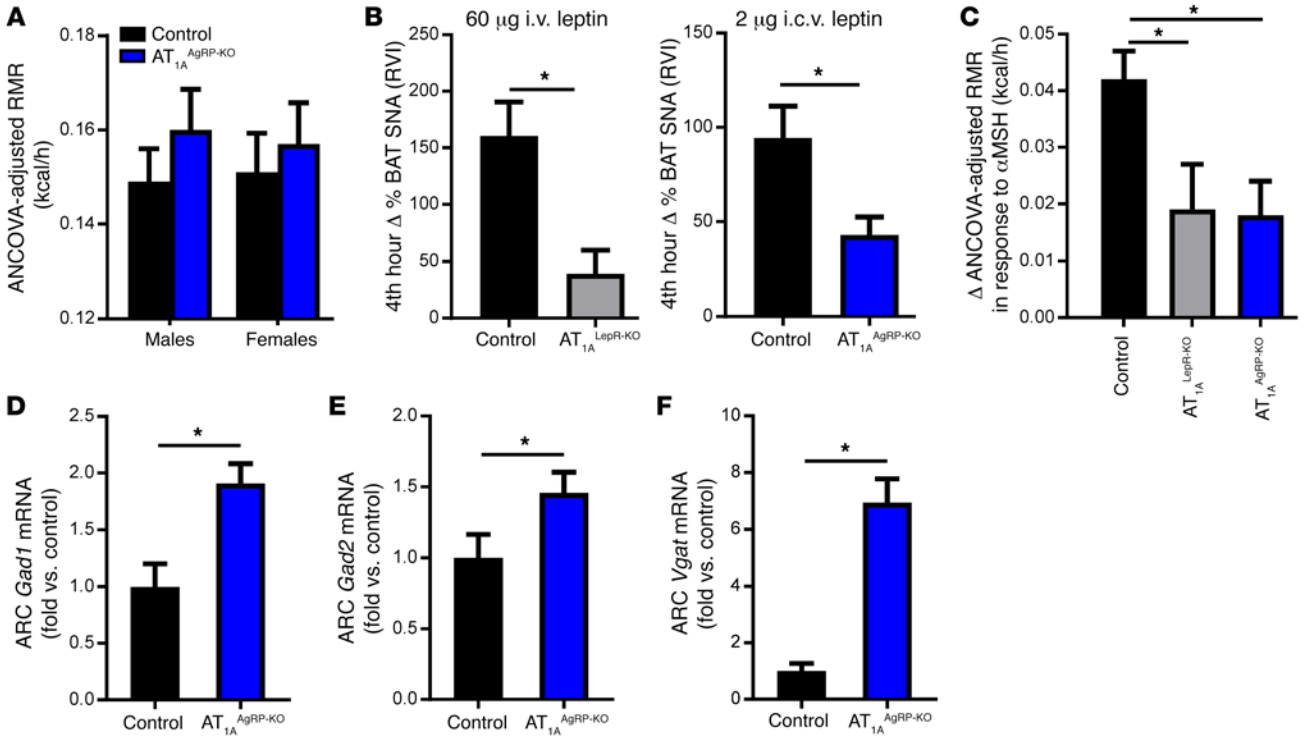

Figure 6. Effect of AT_{1A} receptors on leptin-sensitive AgRP neurons. (**A**) Baseline ANCOVA-adjusted RMR in male and female $AT_{1A}^{AgRP\text{-}KO}$ mice (n = 13 control baseline, n = 13 control αMSH-treated mice; n = 9 chow-fed $AT_{1A}^{LepR\text{-}KO}$ mice; n = 9 αMSH-treated $AT_{1A}^{LepR\text{-}KO}$ mice). (**B**) BAT SNA responses of control, $AT_{1A}^{LepR\text{-}KO}$, and $AT_{1A}^{AgRP\text{-}KO}$ mice to acute leptin injection (60 μg i.v. leptin, n = 6 control mice, n = 5 $AT_{1A}^{LepR\text{-}KO}$ mice; 2 μg i.c.v. leptin, n = 4 control mice, n = 5 $AT_{1A}^{AgRP\text{-}KO}$ mice). (**C**) Changes in ANCOVA-adjusted RMR in response to i.p. administration of αMSH (4.5 μg/g) in control, $AT_{1A}^{LepR\text{-}KO}$, and $AT_{1A}^{AgRP\text{-}KO}$ mice (n = 16 control mice; n = 7 $AT_{1A}^{LepR\text{-}KO}$ mice; n = 9 $AT_{1A}^{AgRP\text{-}KO}$ mice). (**D**–**F**) mRNA for *Gad1* (**D**), *Gad2* (**E**), and *Vgat* (**F**) in the ARC of male control and $AT_{1A}^{AgRP\text{-}KO}$ mice after a chow diet (n = 10 control mice, n = 5 $AT_{1A}^{AgRP\text{-}KO}$ mice). Data represent the mean ± SEM. *P < 0.05, by Tukey's multiple comparisons procedure.

mice, as $VGAT^{AgRP\text{-}KO}$ animals were resistant to HFD-induced weight gain selectively due to an elevated RMR (23). As it has been demonstrated that expression of glutamate decarboxylase enzyme 1 (GAD1) (also known as GAD67) positively correlates with GABA release (25), we examined the expression of GABA synthetic enzymes within the ARC. mRNA levels for both of the glutamate decarboxylase enzymes *Gad1* and *Gad2* (also known as GAD65) (Figure 6, D and E) and *Vgat* (Figure 6F) were significantly increased in $AT_{1A}^{AgRP\text{-}KO}$ mice compared with mRNA levels in littermate controls. Further, $AT_{1A}^{LepR\text{-}KO}$ mice showed similar increases in *Gad1* and *Gad2* levels in the ARC (*Gad1*, 1.5-fold increase, $P < 0.05$; *Gad2*, 1.6-fold increase, $P < 0.05$). Together, these findings support a role for AT_{1A} within ARC AgRP neurons in the control of GABA signaling.

Discussion

Our current study underscores a major role of the RAS within the brain in the control of energy homeostasis. This is mediated in large part through actions of ANG II upon AT_{1A}, localized to a subset of LEPR-expressing neurons within the ARC that also express AgRP. These AT_{1A} receptors are required for ANG II and leptin to fully stimulate SNA and RMR, but not BP. These AT_{1A} receptors appear to tonically suppress GABA expression, and thus angiotensinergic stimulation of the ARC ultimately results in the stimulation of SNA and the RMR through the disinhibition of POMC and αMSH stimulation of second-order neurons (Figure 7).

It is well established that the CNS develops resistance to leptin during obesity. More recently, it has been suggested that this resistance is selective, whereby the cardiovascular effects of leptin remain intact, while the metabolic effects of leptin are abolished (26). Current research on the mechanisms underlying selective leptin resistance (SLR) focuses on deficits in leptin signaling. However, our data support a possible role for central ANG II signaling in SLR, as we have shown that ANG II AT_{1A} receptors specifically in leptin-sensitive cells are dispensable for BP control, but necessary for RMR control and thus energy balance. The general concept that AT_1 receptors mediate leptin sensitivity is also supported in a recent study by Müller-Fielitz et al. (27). In contrast to the effects observed in our studies, it was demonstrated that peripheral treatment with the AT_1 antagonist telmisartan prevented leptin resistance in rats fed a high-calorie/cafeteria diet (27). Further, TGR(ASrAOGEN) rats, which exhibit glial-specific knockdown of angiotensinogen expression, are small and resistant to weight gain with high-calorie diets (28). It is unclear how species differences, peripheral actions of telmisartan, and developmental or receptor sensitivity changes in the TGR(ASrAOGEN) rats (29) may complicate the interpretation of these studies in concert with the current study. In addition, we and others have documented interacting but opposing effects of the brain versus the peripheral RAS in the control of the RMR (9, 19, 30–33). Thus, further elucidation of site-, receptor-, and second-messenger–specific actions of ANG II within the brain and

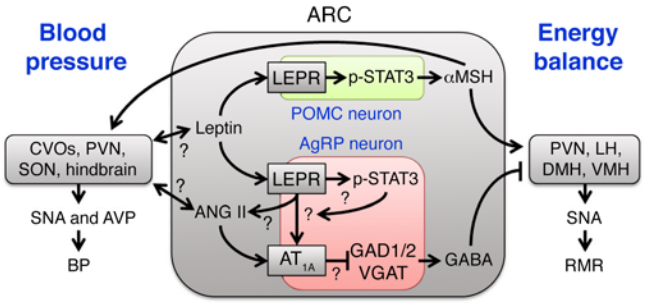

Figure 7. Working model. Working model illustrating circuits within the ARC informed by the current study. See also Supplemental Figure 3 for an anatomical illustration of the relevant brain regions. AVP, arginine vasopressin; CVOs, circumventricular organs.

periphery in the control of leptin sensitivity and cardiovascular and metabolic function is warranted.

An anatomical dissociation of cardiovascular versus metabolic control mechanisms by leptin has been previously implied by other studies. Supporting the idea of possible cross-talk between leptin and ANG II in other brain regions, Smith et al. demonstrated that the SFO of young Sprague-Dawley rats responds to leptin with induction of p-STAT3 and that a large fraction of neurons from this region exhibit altered excitability in response to leptin (34). Young et al. demonstrated that i.c.v. delivery to *Lepr*$^{fl/fl}$ mice of an adenovirus encoding Cre-recombinase, which provides surprisingly specific targeting of the SFO, abolished renal SNA responses to peripheral or central leptin administration, while similar disruption of the AT_{1A} receptor abolished BAT SNA responses to leptin (35, 36). As the SFO is a well-characterized target for cardiovascular control by ANG II, it is intriguing that LEPR appears to be present in this region and that its disruption selectively modulates cardiovascular but not metabolic control, while disruption of AT_{1A} in this region attenuates metabolic responses to leptin. In the current study, we detected tdTomato reporter expression in the SFO of *Lepr-Cre ROSA-stop*^{flox}*-tdTomato* NZ44 mice, but no overlap with the GFP reporter (Figure 2A), which may indicate that the LEPR and AT_{1A} receptors are present in distinct neurons of this brain region in mice. Further, this lack of colocalization in the SFO may explain the lack of BP effect in $AT_{1A}^{LepR\text{-}KO}$ mice (Figure 4B).

It is likely that leptin signaling contributes to the transcriptional regulation of RAS signaling components. Indeed, i.c.v. administration of leptin leads to elevated AT_{1A} receptor expression in the ARC, and *ob/ob* mice have decreased expression and activity of angiotensin-converting enzyme (ACE) (15, 37, 38). Further, administration of leptin to *ob/ob* mice enhances plasma RAS expression (37, 38), and angiotensinogen is expressed in AgRP neurons of the ARC (21). Leptin-activated second-messenger pathways, such as p-STAT3, have also been shown to promote the transcription of angiotensinogen in other cell types (39–44). In addition, i.c.v. administration of the ACE inhibitor captopril attenuates SNA responses to central leptin (15). Thus, it is reasonable to hypothesize that leptin signaling may activate an autocrine RAS signaling mechanism within AgRP neurons of the ARC, ultimately to control the RMR.

In conclusion, our data demonstrate a critical requirement of the ANG II AT_{1A} receptor, specifically localized to leptin-sensitive AgRP neurons, in the control of RMR. This functional interaction appears to be specific to the control of RMR and may therefore contribute to the development of SLR. The results presented here illustrating a selective effect of AT_{1A} in AgRP neurons upon RMR, but not ingestive behavior, also raise the intriguing possibility that a specific subset of AgRP neurons expressing AT_{1A} contribute to RMR control. In contrast, AT_{1A} signaling may not be functional within the AgRP neurons that contribute to ingestive behavior. Further exploration of each of these novel concepts is warranted.

Methods

Animal subjects. The $AT_{1A}^{LepR\text{-}KO}$ colony was maintained on a C57BL/6J background by iterative breeding of a male mouse expressing Cre recombinase under control of the *Lepr* promoter (12) with a female mouse with loxP sites flanking the *AT1a* allele (JAX-016211; The Jackson Laboratory) (45). The $AT_{1A}^{AgRP\text{-}KO}$ colony was maintained on a C57BL/6J background by iterative breeding of a male mouse expressing Cre recombinase under control of the *Agrp* promoter (JAX-012899; The Jackson Laboratory) with a female mouse with loxP sites flanking the *AT1a* allele. Experiments were conducted in 10- to 15-week-old male and female mice. Littermate controls were used throughout, and no differences for any endpoint were discovered when comparing among littermate controls of various genotypes (see the Supplemental Data for additional details regarding the littermate controls). Mice were housed at 25°C on a standard 12-hour light/12-hour dark cycle with ad libitum access to water and standard chow (18% kcal from fat; Teklad diet 7013; Envigo) or an HFD (45% kcal from fat; OpenSource diet D12451; Research Diets Inc.). Inbred male C57BL/6J and *db/db* mice (JAX-000642) maintained on the C57BL/6J background were obtained from The Jackson Laboratory. NZ44 mice backcrossed onto the C57BL/6J background (originally derived by the GENSAT Project at The Rockefeller University, New York, New York, USA) were obtained from Teresa Milner's laboratory at Weill Cornell Medical College (New York, New York, USA) (11).

Intracerebroventricular delivery of ANG II. Mice were instrumented with an i.c.v. cannula (ALZET Brain Infusion Kit III) connected to an osmotic minipump (ALZET Model 1004) for chronic i.c.v. administration of aCSF (Tocris; 3525) or ANG II (5 ng/h; Sigma-Aldrich; A9525). Under anesthesia with i.p. ketamine/xylazine, the mice were placed in a stereotaxic frame, the minipump was inserted under the skin, and the cannula was implanted using the following coordinates: 1.1 mm lateral, 0.5 mm caudal to bregma, and 3.0 mm ventral from the surface of the skull. The cannula was secured to the skull using Vetbond (3M) and dental cement.

DOCA-salt model. A 50-mg pellet of DOCA (Sigma-Aldrich) was implanted into the s.c. cavity under isoflurane anesthesia. Animals were subsequently singly housed and allowed ad libitum access to standard chow and both tap water and 0.15 M NaCl water for 3 weeks.

Brain punches. Mice were euthanized and brains were harvested, frozen in 2-methylbutane and then in embedding medium (Tissue-Tek O.C.T. Compound; Sakura Finetek), and stored at –80°C. Coronal sections (50-μm) of the brain were cut using a cryostat, and micropunches of the cortex and SFO were obtained using a 0.75-mm needle (Stoelting). Bilateral punches of the PVN, ARC, and SON were taken using 0.50-mm and 0.75-mm needles, respectively. Genomic DNA was isolated using the AllPrep DNA/RNA Micro Kit (QIAGEN; catalog 80284), and Cre-mediated recombination was

examined by PCR using Taq Platinum (Invitrogen, Thermo Fisher Scientific). *AT1a* gene primers were designed to produce a 2,761-bp band for the intact *AT1a* gene or a 309-bp band for the recombined fragment, because of the excision of exon 3 as previously described (46). Total RNA was isolated from brain punches by TRIzol (Thermo Fisher Scientific) extraction, and cDNA was made using SuperScript III Reverse Transcriptase (Invitrogen, Thermo Fisher Scientific). Real-time quantitative PCR for mouse *Pomc*, *Agrp*, *Gad1*, *Gad2*, *Vgat*, and actin was performed using TaqMan Gene Expression Assays (Life Technologies, Thermo Fisher Scientific; Mm00435874_m1, Mm00475829_g1, Mm04207432_g1, Mm00484623_m1, and Mm00494138_m1, respectively), and gene expression levels were compared using the Livak method (47).

SNA recording. BAT sympathetic nerves were recorded under α-chloralose anesthesia as previously described (15, 30). Briefly, animals were anesthetized and instrumented with a colonic temperature probe. Cannulae were implanted into the common carotid artery (to record BP) and jugular vein (for i.v. injections). A sympathetic nerve subserving BAT was isolated and suspended on 36-gauge platinum-iridium electrodes and secured with silicone gel. Electrodes were interfaced to a high-impedance probe (HIP-511; Grass Instruments), and the neural signal from BAT was amplified 100,000 times (1×10^5), filtered at low- and high-frequency cutoffs of 100 and 1,000 Hz, respectively, and routed to a resetting voltage integrator (B600c; University of Iowa Bioengineering). Data were recorded using an ADInstruments PowerLab with the associated Chart software.

Home cage experiments. Mice were singly housed in home cages, and standard bedding was replaced by an absorbent pad to facilitate the measurement of food intake and collection of feces at both 10 and 15 weeks of age. Mice were acclimated to the cages for 72 hours before data collection. Body mass and food intake measurements and feces collection were done at the same time daily for 4 days. Energy per gram feces was determined by bomb calorimetry as previously described (48, 49). This energy was applied to feces and food intake to determine energy intake and output, and thus caloric absorption.

RMR. The RMR was determined using respirometry as described previously (19, 30, 46, 50). Briefly, mice were placed into thermally controlled, air-tight chambers maintained at thermoneutrality (30°C), and oxygen consumption and carbon dioxide content of effluent air (flowing at 300 ml/min, corrected to standard temperature and pressure) were continually recorded (AEI analyzers, logged using an ADInstruments PowerLab with the associated Chart software). Analyzers were calibrated daily using soda lime and calibration gas (Praxair). To determine the effect of αMSH treatment on the RMR, baseline RMR measurements were taken in the morning and again in the afternoon following i.p. injection of αMSH.

BP by radiotelemetry. BP and heart rate were assessed using radiotelemetric BP probes (DSI; model TA11PA-C10), with cannulae implanted into the common carotid artery, as previously described (19). Briefly, probes were implanted under ketamine/xylazine anesthesia, and animals were allowed to recover for at least 1 week before 3 consecutive 24-hour periods were recorded (baseline). Data were recorded for 30 seconds every 5 minutes during the recording period and averaged across days within subject before statistical comparisons were made across groups.

Body composition. Body composition was determined using nuclear magnetic resonance (NMR) (Bruker; LF90) as previously described (49–52). Awake animals were lightly restrained in a polycarbonate tube during the 1-minute recording and then immediately placed back into home cages.

IHC. Brain tissue used for IHC was perfused with 4% PFA and incubated in 30% sucrose. Coronal sections (40-μm) were cut using a frozen sledge microtome (American Optical Scientific Instruments), and primary antibodies were added to free-floating sections at 4°C overnight. After washing with 1× PBS, secondary antibodies were added at room temperature for 1 hour. p-STAT3 staining was performed as previously described (53). Briefly, mice were fasted overnight and administered 1 μg/g leptin i.p. the following morning. Thirty minutes later, mice were perfused, and brains were sectioned as described above. Free-floating sections were incubated with the primary antibody for 72 hours, followed by incubation with the secondary antibody for 1 hour. All sections were mounted onto microscope slides and viewed using a Nikon Labophot 2 microscope. Quantification was performed using ImageJ (NIH). The following primary antibodies were used: chicken GFP (Aves Lab Inc., GFP-1010); ACTH (Harbor-UCLA Research and Education Institute); and p-STAT3 (Cell Signaling Technology; 9131S). The following secondary antibodies were used: Alexa Fluor 488 goat anti-chicken (Life Technologies, Thermo Fisher Scientific; A11039); Alexa Fluor 488 goat anti-rabbit (Thermo Fisher Scientific; A11008); and Alexa Fluor 568 goat anti-rabbit (Thermo Fisher Scientific; A11011).

FISH. Mice were euthanized and brain tissue was collected and frozen in 2-methylbutane and then in embedding medium (Tissue-Tek O.C.T. Compound; Sakura Finetek) and stored at –80°C. Next, 10-μm coronal sections were cut using a cryostat and underwent the RNAscope Multiplex FISH protocol for fresh-frozen tissue (Advanced Cell Diagnostics). Briefly, sections were pretreated with protease IV, followed by hybridization with target probes, which contained 20 double Z oligo probe pairs for the specific RNA target of interest (*Agtr1a*, 404001; AgRP, 400711; and POMC, 314081). Subsequent hybridization was completed with RNAscope detection reagents to amplify the fluorescent signal. All images were captured using a Leica STED 3× at ×20 to ×40 magnification.

Statistics. All quantitative data were analyzed using the 2-tailed Student's *t* test, ANOVA, or analysis of covariance (ANCOVA), followed by Tukey's multiple comparisons procedures. All experimental results passed tests of normal distribution and equal variance, so only parametric analyses are reported. Gene expression data were analyzed using the Livak method (47). Data are reported as the mean ± SEM throughout, and a *P* value of less than 0.05 was used as the threshold for statistical significance.

Study approval. All animal experiments were approved by the IACUC of the University of Iowa.

Author contributions

KEC and JLG conceptualized the project and drafted and revised the manuscript. KEC, JAS, AML, BJW, NKL, CMLB, NAP, DAM, KNGC, and KR collected and analyzed data and revised the manuscript.

Acknowledgments

The authors acknowledge the intellectual assistance of Curt D. Sigmund, Allyn L. Mark (both from University of Iowa, Iowa City, Iowa), Robin L. Davisson (Cornell University, Ithaca, New York), Martin D. Cassell, and Robert D. Roghair and the technical assis-

tance of Deborah R. Davis and Mariah R. Leidinger (all from University of Iowa, Iowa City, Iowa). Fellowship support was obtained from the American Heart Association (16PRE30980043, to JAS, 14PRE20380401, to KEC and 14PRE18330015, to NKL); the NIH (GM067795, to JAS); the American Physiological Society (to BJW); the University of Iowa Center for Research by Undergraduates (to BJW); and the University of Iowa Medical Student Research Program (to CMLB). The project was supported by grants from the NIH (HL084207, HL098276, and HL134850); the American Heart Association (15SFRN23730000); the American Diabetes Association (1-14-BS-079); the University of Iowa Office of the Vice President for Research and Economic Development; and the Fraternal Order of Eagles Diabetes Research Center (to KR and JLG).

Address correspondence to: Justin L. Grobe, Department of Pharmacology, University of Iowa, 51 Newton Rd., 2-307 BSB, Iowa City, Iowa 52242, USA. Phone: 319.353.5789; E-mail: justin-grobe@uiowa.edu.

1. Lavoie JL, Sigmund CD. Minireview: overview of the renin-angiotensin system — an endocrine and paracrine system. *Endocrinology*. 2003;144(6):2179–2183.
2. Dinh DT, Frauman AG, Johnston CI, Fabiani ME. Angiotensin receptors: distribution, signalling and function. *Clin Sci*. 2001;100(5):481–492.
3. Karnik SS, et al. International union of basic and clinical pharmacology. *Pharmacol Rev*. 2015;67(4):754–819.
4. Aldred GP, Chai SY, Song K, Zhuo J, MacGregor DP, Mendelsohn FA. Distribution of angiotensin II receptor subtypes in the rabbit brain. *Regul Pept*. 1993;44(2):119–130.
5. Jöhren O, Sanvitto GL, Egidy G, Saavedra JM. Angiotensin II AT1A receptor mRNA expression is induced by estrogen-progesterone in dopaminergic neurons of the female rat arcuate nucleus. *J Neurosci*. 1997;17(21):8283–8292.
6. McKinley MJ, Allen AM, Clevers J, Paxinos G, Mendelsohn FA. Angiotensin receptor binding in human hypothalamus: autoradiographic localization. *Brain Res*. 1987;420(2):375–379.
7. Sapru HN. Role of the hypothalamic arcuate nucleus in cardiovascular regulation. *Auton Neurosci*. 2013;175(1–2):38–50.
8. do Carmo JM, da Silva AA, Cai Z, Lin S, Dubinion JH, Hall JE. Control of blood pressure, appetite, and glucose by leptin in mice lacking leptin receptors in proopiomelanocortin neurons. *Hypertension*. 2011;57(5):918–926.
9. Claflin KE, Grobe JL. Control of energy balance by the brain renin-angiotensin system. *Curr Hypertens Rep*. 2015;17(5):38.
10. de Kloet AD, et al. Angiotensin type 1a receptors in the paraventricular nucleus of the hypothalamus protect against diet-induced obesity. *J Neurosci*. 2013;33(11):4825–4833.
11. Gonzalez AD, et al. Distribution of angiotensin type 1a receptor-containing cells in the brains of bacterial artificial chromosome transgenic mice. *Neuroscience*. 2012;226:489–509.
12. DeFalco J, et al. Virus-assisted mapping of neural inputs to a feeding center in the hypothalamus. *Science*. 2001;291(5513):2608–2613.
13. Plum L, et al. Enhanced leptin-stimulated Pi3k activation in the CNS promotes white adipose tissue transdifferentiation. *Cell Metab*. 2007;6(6):431–445.
14. Guo DF, et al. The BBSome controls energy homeostasis by mediating the transport of the leptin receptor to the plasma membrane. *PLoS Genet*. 2016;12(2):e1005890.
15. Hilzendeger AM, et al. A brain leptin-renin angiotensin system interaction in the regulation of sympathetic nerve activity. *Am J Physiol Heart Circ Physiol*. 2012;303(2):H197–H206.
16. Itaya Y, Suzuki H, Matsukawa S, Kondo K, Saruta T. Central renin-angiotensin system and the pathogenesis of DOCA-salt hypertension in rats. *Am J Physiol*. 1986;251(2 pt 2):H261–H268.
17. Kubo T, Yamaguchi H, Tsujimura M, Hagiwara Y, Fukumori R. Blockade of angiotensin receptors in the anterior hypothalamic preoptic area lowers blood pressure in DOCA-salt hypertensive rats. *Hypertens Res*. 2000;23(2):109–118.
18. Park CG, Leenen FH. Effects of centrally administered losartan on deoxycorticosterone-salt hypertension rats. *J Korean Med Sci*. 2001;16(5):553–557.
19. Grobe JL, et al. Angiotensinergic signaling in the brain mediates metabolic effects of deoxycorticosterone (DOCA)-salt in C57 mice. *Hypertension*. 2011;57(3):600–607.
20. Quigley JE, et al. Obesity induced renal oxidative stress contributes to renal injury in salt-sensitive hypertension. *Clin Exp Pharmacol Physiol*. 2009;36(7):724–728.
21. Henry FE, Sugino K, Tozer A, Branco T, Sternson SM. Cell type-specific transcriptomics of hypothalamic energy-sensing neuron responses to weight-loss. *Elife*. 2015;4:e09800.
22. Hoggard N, Rayner DV, Johnston SL, Speakman JR. Peripherally administered [Nle4,D-Phe7]-α-melanocyte stimulating hormone increases resting metabolic rate, while peripheral agouti-related protein has no effect, in wild type C57BL/6 and ob/ob mice. *J Mol Endocrinol*. 2004;33(3):693–703.
23. Tong Q, Ye CP, Jones JE, Elmquist JK, Lowell BB. Synaptic release of GABA by AgRP neurons is required for normal regulation of energy balance. *Nat Neurosci*. 2008;11(9):998–1000.
24. Vong L, Ye C, Yang Z, Choi B, Chua S, Lowell BB. Leptin action on GABAergic neurons prevents obesity and reduces inhibitory tone to POMC neurons. *Neuron*. 2011;71(1):142–154.
25. Dicken MS, Hughes AR, Hentges ST. Gad1 mRNA as a reliable indicator of altered GABA release from orexigenic neurons in the hypothalamus. *Eur J Neurosci*. 2015;42(9):2644–2653.
26. Mark AL. Selective leptin resistance revisited. *Am J Physiol Regul Integr Comp Physiol*. 2013;305(6):R566–R581.
27. Müller-Fielitz H, Lau M, Geißler C, Werner L, Winkler M, Raasch W. Preventing leptin resistance by blocking angiotensin II AT1 receptors in diet-induced obese rats. *Br J Pharmacol*. 2015;172(3):857–868.
28. Winkler M, et al. The brain renin-angiotensin system plays a crucial role in regulating body weight in diet-induced obesity in rats. *Br J Pharmacol*. 2016;173(10):1602–1617.
29. Monti J, Schinke M, Böhm M, Ganten D, Bader M, Bricca G. Glial angiotensinogen regulates brain angiotensin II receptors in transgenic rats TGR(ASrAOGEN). *Am J Physiol Regul Integr Comp Physiol*. 2001;280(1):R233–R240.
30. Grobe JL, et al. The brain Renin-angiotensin system controls divergent efferent mechanisms to regulate fluid and energy balance. *Cell Metab*. 2010;12(5):431–442.
31. Grobe JL, Rahmouni K, Liu X, Sigmund CD. Metabolic rate regulation by the renin-angiotensin system: brain vs. body. *Pflugers Arch*. 2013;465(1):167–175.
32. Littlejohn NK, Grobe JL. Opposing tissue-specific roles of angiotensin in the pathogenesis of obesity, and implications for obesity-hypertension. *Am J Physiol Regul Integr Comp Physiol*. 2015;309(12):R1463–R1473.
33. Littlejohn NK, et al. Suppression of resting metabolism by the angiotensin AT2 receptor. *Cell Rep*. 2016;16(6):1548–1560.
34. Smith PM, et al. The subfornical organ: a central nervous system site for actions of circulating leptin. *Am J Physiol Regul Integr Comp Physiol*. 2009;296(3):R512–R520.
35. Young CN, Morgan DA, Butler SD, Mark AL, Davisson RL. The brain subfornical organ mediates leptin-induced increases in renal sympathetic activity but not its metabolic effects. *Hypertension*. 2013;61(3):737–744.
36. Young CN, et al. Angiotensin type 1a receptors in the forebrain subfornical organ facilitate leptin-induced weight loss through brown adipose tissue thermogenesis. *Mol Metab*. 2015;4(4):337–343.
37. Hilzendeger AM, et al. Leptin regulates ACE activity in mice. *J Mol Med*. 2010;88(9):899–907.
38. Hilzendeger AM, et al. Autonomic dysregulation in ob/ob mice is improved by inhibition of angiotensin-converting enzyme. *J Mol Med*. 2010;88(4):383–390.
39. Mascareno E, Dhar M, Siddiqui MA. Signal transduction and activator of transcription (STAT) protein-dependent activation of angiotensinogen promoter: a cellular signal for hypertrophy in cardiac muscle. *Proc Natl Acad Sci U S A*. 1998;95(10):5590–5594.
40. Mascareno E, Siddiqui MA. The role of Jak/STAT signaling in heart tissue renin-angiotensin system. *Mol Cell Biochem*. 2000;212(1–2):171–175.
41. Fukuzawa J, et al. Cardiotrophin-1 increases angiotensinogen mRNA in rat cardiac myocytes through STAT3: an autocrine loop for hypertrophy. *Hypertension*. 2000;35(6):1191–1196.

42. Sherman CT, Brasier AR. Role of signal transducers and activators of transcription 1 and -3 in inducible regulation of the human angiotensinogen gene by interleukin-6. *Mol Endocrinol*. 2001;15(3):441–457.
43. Ray S, Sherman CT, Lu M, Brasier AR. Angiotensinogen gene expression is dependent on signal transducer and activator of transcription 3-mediated p300/cAMP response element binding protein-binding protein coactivator recruitment and histone acetyltransferase activity. *Mol Endocrinol*. 2002;16(4):824–836.
44. Qi Y, et al. Novel mechanism of blood pressure regulation by forkhead box class O1-mediated transcriptional control of hepatic angiotensinogen. *Hypertension*. 2014;64(5):1131–1140.
45. Rateri DL, et al. Endothelial cell-specific deficiency of Ang II type 1a receptors attenuates Ang II-induced ascending aortic aneurysms in LDL receptor$^{-/-}$ mice. *Circ Res*. 2011;108(5):574–581.
46. Hilzendeger AM, et al. Angiotensin type 1a receptors in the subfornical organ are required for deoxycorticosterone acetate-salt hypertension. *Hypertension*. 2013;61(3):716–722.
47. Livak KJ, Schmittgen TD. Analysis of relative gene expression data using real-time quantitative PCR and the 2(–ΔΔC(T)) Method. *Methods*. 2001;25(4):402–408.
48. Fink BD, et al. A mitochondrial-targeted coenzyme q analog prevents weight gain and ameliorates hepatic dysfunction in high-fat-fed mice. *J Pharmacol Exp Ther*. 2014;351(3):699–708.
49. Bahra SM, et al. Risperidone-induced weight gain is mediated through shifts in the gut microbiome and suppression of energy expenditure. *EBioMedicine*. 2015;2(11):1725–1734.
50. Weidemann BJ, et al. Dietary sodium suppresses digestive efficiency via the renin-angiotensin system. *Sci Rep*. 2015;5:11123.
51. Burnett CM, Grobe JL. Direct calorimetry identifies deficiencies in respirometry for the determination of resting metabolic rate in C57Bl/6 and FVB mice. *Am J Physiol Endocrinol Metab*. 2013;305(7):E916–E924.
52. Burnett CM, Grobe JL. Dietary effects on resting metabolic rate in C57BL/6 mice are differentially detected by indirect (O_2/CO_2 respirometry) and direct calorimetry. *Mol Metab*. 2014;3(4):460–464.
53. Cui H, et al. Neuroanatomy of melanocortin-4 receptor pathway in the lateral hypothalamic area. *J Comp Neurol*. 2012;520(18):4168–4183.